This article was downloaded by:
On: *14 January 2011*
Access details: *Access Details: Free Access*
Publisher *Taylor & Francis*
Informa Ltd Registered in England and Wales Registered Number: 1072954 Registered office: Mortimer House, 37-41 Mortimer Street, London W1T 3JH, UK

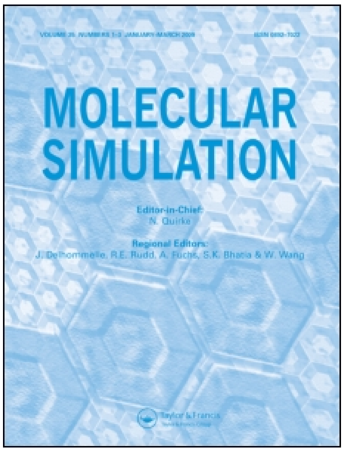

Molecular Simulation

Publication details, including instructions for authors and subscription information:
http://www.informaworld.com/smpp/title~content=t713644482

Some aspects of the Methodology in Gibbs Ensemble Monte Carlo Simulations in Connection with a Model Fluid of C_{60}

Tamás Kristóf[a]; János Liszi[a]
[a] Department of Physical Chemistry, University of Veszprém, Veszprém, Hungary

To cite this Article Kristóf, Tamás and Liszi, János(1999) 'Some aspects of the Methodology in Gibbs Ensemble Monte Carlo Simulations in Connection with a Model Fluid of C_{60}', Molecular Simulation, 21: 4, 227 — 238
To link to this Article: DOI: 10.1080/08927029908022063
URL: http://dx.doi.org/10.1080/08927029908022063

PLEASE SCROLL DOWN FOR ARTICLE

Full terms and conditions of use: http://www.informaworld.com/terms-and-conditions-of-access.pdf

This article may be used for research, teaching and private study purposes. Any substantial or systematic reproduction, re-distribution, re-selling, loan or sub-licensing, systematic supply or distribution in any form to anyone is expressly forbidden.

The publisher does not give any warranty express or implied or make any representation that the contents will be complete or accurate or up to date. The accuracy of any instructions, formulae and drug doses should be independently verified with primary sources. The publisher shall not be liable for any loss, actions, claims, proceedings, demand or costs or damages whatsoever or howsoever caused arising directly or indirectly in connection with or arising out of the use of this material.

Molecular Simulation, 1999, Vol. 21, pp. 227–238
Reprints available directly from the publisher
Photocopying permitted by license only

Published by license under
the Gordon and Breach Science
Publishers imprint.
Printed in India.

SOME ASPECTS OF THE METHODOLOGY IN GIBBS ENSEMBLE MONTE CARLO SIMULATIONS IN CONNECTION WITH A MODEL FLUID OF C_{60}

TAMÁS KRISTÓF* and JÁNOS LISZI

Department of Physical Chemistry, University of Veszprém,
P.O. Box 158, Veszprém, H-8201, Hungary

(Received May 1998; accepted June 1998)

Conventional and new versions of the Gibbs ensemble Monte Carlo technique existing for one-component systems were applied for the determination of the vapour–liquid coexistence in the model fluid of C_{60}. Employing exact long range corrections for the model, no significant particle number dependence of the simulation results was found. The results confirm that a liquid phase may exist for this model.

Keywords: Monte Carlo; Gibbs ensemble; vapour–liquid equilibrium; fullerene

1. INTRODUCTION

The Gibbs ensemble Monte Carlo (GEMC) technique [1, 2] is specifically developed for molecular-based calculations of fluid phase equilibria. In this technique the required equalities of temperature (T), pressure (p) and chemical potential (μ) between coexisting phases are achieved by performing the calculations in two distinct simulation boxes, each within its own periodic boundary conditions. Each box represents a region deep inside one of the coexisting phases, so the problem with the direct simulation of the interface between the phases can be avoided. The conventional GEMC methods (NVT and NpT versions) incorporate elements of canonical, grand canonical and isothermal-isobaric ensemble simulations; the subsystems are

---

*Corresponding author.

allowed to exchange particles and their volumes are allowed to fluctuate at a specified temperature. Recently novel versions of the GEMC technique were proposed [3, 4] and applied to atomic and site–site interaction model fluids [4–6]. Unlike conventional GEMC methods, the new schemes allow the exchange of heat between the correlated subsystems.

For lack of satisfactory experimental data, the existence of a stable liquid phase of C_{60} fullerene has been investigated by computer simulations and other theoretical studies [7–10]. At high temperatures the C_{60} molecules rotate freely and can be approximated by spheres. The interactions between the molecules can be realistically modelled by an effective pair potential which consists of a harshly repulsive soft sphere and a rapidly decaying attractive part with a deep minimum [11]. This pair potential was constructed by assuming that the carbon atoms in two different C_{60} molecules interact through a Lennard-Jones potential and these interactions can be integrated over the surfaces of two spheres.

To our knowledge the latest computer simulation study concerning the vapour–liquid coexistence for this model of C_{60} was reported by Caccamo *et al.* [10]. Their results obtained from conventional GEMC simulations indicate that, in a narrow range of temperature, a liquid phase should exist. However, in agreement with other prediction [8], the long range corrections were neglected in this calculations and considerable finite size effects were found. We performed additional GEMC simulations for the model applying exact long range corrections and examined also the particle number dependence of the simulations. Except for the number dependence investigation we used the novel versions of the GEMC technique.

2. METHOD

The partition function of the Gibbs ensemble can be written as a combination of the partition functions of the correlated subsystems noting that the particles do not interact between the subsystems [12]. For one-component systems, the phase rule enables us to specify one of the intensive variables T, p and μ when two phases coexist. Therefore, three possibilities exist [3].

The conventional (NVT) form of the Gibbs ensemble partition function reads

$$Q_{NVT}^{\mathrm{Gibbs}} = \frac{1}{V_0} \sum_{N^{\mathrm{I}}=0}^{N} \int_0^V dV^{\mathrm{I}} Q_{NVT}^{\mathrm{I}} Q_{NVT}^{\mathrm{II}}, \tag{1}$$

where I and II indicate the subsystems, Q represent the dimensionless partition functions, N and V are the total number of particles and the volume of the system, and V_0 is a basic unit of volume chosen to render the Gibbs ensemble partition function dimensionless. Here, $N = N^{\mathrm{I}} + N^{\mathrm{II}}$ and $V = V^{\mathrm{I}} + V^{\mathrm{II}}$ are constrained to be constant. In this simulation, the particle displacement step, which is responsible for the internal equilibrium within each subsystem, is performed according to the canonical (NVT) Monte Carlo rules. In this way, the condition of thermal equilibrium (equalities of T between coexisting phases) can be satisfied. The conditions of mechanical and chemical equilibria (equalities of p and μ between coexisting phases) are fulfilled by performing appropriate volume and particle exchange steps between the subsystems.

When the whole system is considered in the isoenthalpic–isobaric ensemble (NpH version), the dimensionless partition function for the Gibbs ensemble is given by [3, 4]

$$Q_{NpH}^{\mathrm{Gibbs}} = \frac{1}{pV_0} \sum_{N^{\mathrm{I}}=0}^{N} \int_0^H dH^{\mathrm{I}} Q_{NpH}^{\mathrm{I}} Q_{NpH}^{\mathrm{II}}, \tag{2}$$

where the fixed extensive variables are the total number of particles N and the total enthalpy H ($H = H^{\mathrm{I}} + H^{\mathrm{II}}$). In this simulation, the internal equilibrium within each subsystem and the mechanical equilibrium are attained by performing isoenthalpic–isobaric Monte Carlo steps [13]. It can be seen furthermore, that the heat exchange step, which is responsible for the thermal equilibrium, is accomplished by the exchange of enthalpy.

Instead of the temperature or the pressure, the chemical potential of the system can also be specified in advance. In this case the dimensionless partition function for the Gibbs ensemble can be written as [4]

$$Q_{\mu VH}^{\mathrm{Gibbs}} = \frac{1}{\mu V_0} \int_0^L dL^{\mathrm{I}} \int_0^V dV^{\mathrm{I}} Q_{\mu VL}^{\mathrm{I}} Q_{\mu VL}^{\mathrm{II}}, \tag{3}$$

where L is the Hill energy (see, $L = K + U - \mu N$, with K being the kinetic energy and U the potential energy). In this simulation, the internal equilibrium within each subsystem and the chemical equilibrium are attained by performing μVL Monte Carlo steps [13]. The conditions of thermal and mechanical equilibria are satisfied by carrying out appropriate changes in the Hill energies and volumes of the subsystems. Note that the conservation of the total number of particles throughout the simulation is disabled in this scheme.

In the simulations of vapour–liquid coexistence of binary mixtures two intensive variables can be specified, so three additional possibilities exist: either p and T, or μ_1 and T, or μ_1 and p are fixed. Since there are two different ways for implementing the fixed-temperature versions [4], five additional forms of the Gibbs ensemble partition function can be found accordingly.

A detailed description of these versions including also the acceptance probabilities for the different steps can be found elsewhere [2–4].

3. PAIR POTENTIAL MODEL AND COMPUTATIONAL DETAILS

The simplified spherical pair potential of C_{60} is given by [11]

$$\phi(r) = \frac{\varepsilon_R}{s}\left[\frac{1}{(s-1)^9} + \frac{1}{(s+1)^9} - \frac{2}{s^9}\right] - \frac{\varepsilon_A}{s}\left[\frac{1}{(s-1)^3} + \frac{1}{(s+1)^3} - \frac{2}{s^3}\right], \quad (4)$$

where r is the distance between the centres of two fullerene molecules, $s = r/a$ with $a = 0.71$ nm being the diameter of the molecule; $\varepsilon_R = 1.3595 \cdot 10^{-23}$ J and $\varepsilon_A = 7.494 \cdot 10^{-21}$ J are the repulsive and attractive energy parameters. The potential function crosses zero at $\sigma = 0.959$ nm and its well depth is $\varepsilon = 4.46 \cdot 10^{-20}$ J. The character of this pair potential is harshly repulsive at short distances comparing to a Lennard-Jones potential with the same parameters ε and σ. The interaction energy is $\phi(r) = -0.0076 \cdot \varepsilon$ at $r = 2.0 \cdot \sigma$, which shows the short rangedness of this potential considering that, for the Lennard-Jones potential, $\phi(r) = -0.062 \cdot \varepsilon$ at $r = 2.0 \cdot \sigma$. In the case of the Lennard-Jones potential, however, the value of $\phi(r) = -0.0076 \cdot \varepsilon$ is reached already at $r = 2.84 \cdot \sigma$; it is known in the literature [12, 14, 15] that this distance is too short, in general, for obtaining negligible effects in fluid simulations with the Lennard-Jones potential when a spherical truncation without inclusion of the long range correction is used.

GEMC simulations were started from a face-centred cubic lattice configuration or from a configuration of a previous run. An equilibration period of 20 000 cycles were followed by a production period of 100 000 cycles. Depending on the version used, each cycle consisted of N^{I} and N^{II} attempted particle displacements in subsystem I and II, one heat exchange between the subsystems, one coupled or uncoupled volume change of the two subsystems, and particle transfers between the subsystems or between a constant chemical potential bath and each of the subsystems. The type of move to be performed and the particle for the corresponding move were selected at random. The maximum molecular displacements, volume and heat changes were adjusted to obtain, where possible, a 50% acceptance rate for the attempted move. The number of particles to be transferred was chosen to achieve 2 or 3 accepted particle transfers per cycle. For comparison, conventional GEMC simulations (*NVT* version) also were carried out by the above procedure (without the heat exchange step). The constant *N* version GEMC simulations were performed with 512, 1000 or 1500 particles. Estimates of the standard deviations were made by dividing the runs into 10 blocks and calculating the block averages. In order to check that the coexisting phases are clearly separated, densities were monitored and density histograms were constructed. Interactions in both phases employed periodic boundary conditions with a spherical truncation at half the box length. Assuming that the pair distribution function is equal to 1 outside of this sphere, the usual long range corrections were applied to the energy, pressure and chemical potential [15]. For example, the long range part of the potential energy is given by

$$U_{LRC} = 2\pi N\rho a^3 \left\{ \varepsilon_R \left[\frac{1}{7(s_c-1)^7} + \frac{1}{8(s_c-1)^8} + \frac{1}{7(s_c+1)^7} - \frac{1}{8(s_c+1)^8} - \frac{2}{7s_c^7} \right] - \varepsilon_A \left[\frac{1}{s_c-1} + \frac{1}{2(s_c-1)^2} + \frac{1}{s_c+1} - \frac{1}{2(s_c+1)^2} - \frac{2}{s_c} \right] \right\}, \tag{5}$$

where ρ is the number density and $s_c = r_c/a$ with r_c being the cut-off distance.

4. RESULTS AND DISCUSSION

The results of the present study are summarized in Table I, where also the average number of particles ($\langle N^L \rangle$ and $\langle N^V \rangle$) for both simulation boxes are displayed. The main results are shown also in Figure 1. Only the statistical uncertainties of the number densities are illustrated here for clarity purposes. The equilibrium quantities are compared to the data reported by Caccamo *et al.* [10]. Following the usual convention for the pressure and chemical potential (residual chemical potential plus $RT \cdot \ln \rho$ term),

TABLE I Vapour–liquid coexistence data for the model of fullerene obtained from the different versions of GEMC method. The liquid and vapour phases are labelled by L and V, respectively. The numbers in parentheses represent the statistical uncertainties in the last digits

Version	$\langle N^L \rangle$	$\langle N^V \rangle$	$\langle T \rangle / K$	$\langle p \rangle / bar$	$-\langle U^L \rangle / kJ/mol$	$-\langle U^V \rangle / kJ/mol$	$\langle \rho^L \rangle / nm^{-3}$	$\langle \rho^V \rangle / nm^{-3}$	$-\langle \mu \rangle / kJ/mol$
NpH	268(9)	244(9)	1637(14)	8.38	90.1(16)	6.7(3)	0.960(14)	0.045(1)	61.2(2)
NpH	261(4)	251(4)	1694(8)	11.31	85.5(9)	8.7(2)	0.924(8)	0.062(1)	60.2(2)
NVT[11]	561(8)	39(8)	1700	11.4(8)	84.0(7)	8.4(9)	0.911(7)	0.063(6)	
NVT[11]	1412(10)	88(10)	1700	11.1(7)	84.5(6)	8.4(8)	0.914(7)	0.061(6)	
μVL	240(10)	258(3)	1702(4)	11.3(1)	84.5(8)	8.6(1)	0.915(7)	0.062(1)	60.1
NpH	268(6)	244(6)	1753(12)	14.24	79.9(8)	10.7(3)	0.874(12)	0.080(1)	59.7(3)
μVL	256(23)	270(9)	1789(5)	16.5(4)	76.1(9)	12.3(4)	0.839(9)	0.095(2)	59.2
NpH	265(14)	247(14)	1799(13)	17.80	74.7(22)	13.4(6)	0.826(5)	0.105(4)	58.9(3)
NVT[11]	538(4)	62(4)	1800	17.8(5)	74.8(7)	13.0(7)	0.827(1)	0.104(6)	
μVL	325(30)	225(12)	1824(7)	19.5(5)	72.5(12)	14.7(6)	0.804(13)	0.118(5)	58.6
NVT[11]	517(15)	83(15)	1825	19.9(10)	71.5(9)	15.1(12)	0.794(10)	0.124(12)	
NpH	245(10)	267(10)	1844(9)	21.36	70.3(13)	16.5(9)	0.782(15)	0.134(7)	58.3(3)
NVT[11]	519(8)	81(8)	1850	21.3(8)	67.3(11)	15.5(8)	0.746(17)	0.131(10)	
NVT[11]	1230(23)	270(23)	1850	22.0(8)	69.4(5)	16.7(10)	0.772(5)	0.139(8)	
NVT	415(14)	97(14)	1850	21.7(11)	69.2(15)	16.3(16)	0.768(18)	0.137(14)	58.4(5)
NVT	260(17)	252(17)	1850	22.2(7)	68.6(17)	17.2(8)	0.763(21)	0.141(7)	58.1(3)
NVT	487(54)	513(54)	1850	22.1(9)	69.1(13)	17.5(16)	0.768(16)	0.143(12)	58.1(4)
μVL	252(22)	254(12)	1857(4)	22.6(5)	68.9(14)	17.7(7)	0.767(15)	0.145(5)	58.2
NVT[11]	514(12)	86(12)	1870	23.1(7)	64.7(11)	16.7(11)	0.716(30)	0.143(12)	
NpH	256(12)	256(12)	1871(9)	24.29	67.0(22)	18.8(5)	0.747(27)	0.159(4)	57.9(3)
NVT[11]	511(19)	89(19)	1880	24.3(5)	62.4(16)	17.9(7)	0.687(30)	0.156(10)	
NVT	251(23)	261(23)	1880	25.3(7)	65.6(16)	20.5(15)	0.732(19)	0.173(12)	57.8(3)
NVT	812(19)	188(19)	1880	24.7(8)	65.1(12)	19.4(11)	0.722(16)	0.164(11)	58.0(3)
NVT	488(46)	512(46)	1880	24.9(7)	64.4(14)	20.3(13)	0.714(17)	0.171(11)	57.8(3)
NVT	1024(41)	476(41)	1880	24.7(7)	65.0(16)	19.8(12)	0.721(19)	0.166(10)	57.9(3)
μVL	270(29)	251(17)	1892(9)	26.1(7)	63.6(23)	21.5(12)	0.708(28)	0.183(7)	57.6
NVT[11]	510(30)	90(30)	1890	25.6(8)	60.2(9)	19.2(14)	0.656(50)	0.168(15)	

NVT[11]	1137(46)	363(46)	1890	26.0(6)	63.4(12)	21.5(15)	0.700(25)	0.182(13)	
NVT	419(11)	93(11)	1890	25.7(7)	62.9(13)	20.0(12)	0.697(20)	0.174(11)	57.9(3)
NVT	265(20)	247(20)	1890	26.0(8)	62.3(27)	21.2(12)	0.690(35)	0.182(10)	57.6(3)
NVT	501(27)	499(27)	1890	26.1(4)	63.0(15)	21.6(9)	0.698(20)	0.182(7)	57.6(3)
NpH	255(20)	257(20)	1894(9)	26.38	63.8(22)	20.9(20)	0.712(26)	0.182(12)	57.7(3)
NVT[11]	405(32)	105(32)	1910	28.6(10)	56.6(21)	22.2(16)	0.616(41)	0.207(26)	
NpH	261(16)	251(16)	1916(6)	28.60	58.7(21)	22.4(7)	0.650(26)	0.197(5)	57.6(3)

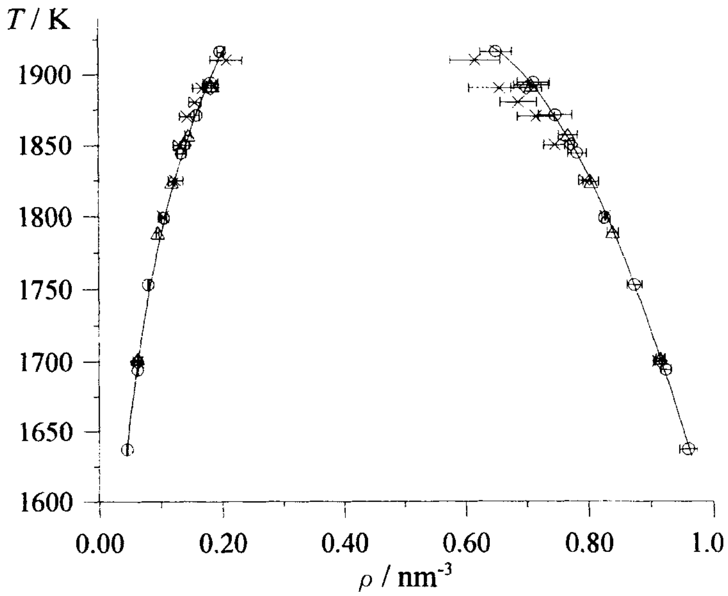

FIGURE 1 Orthobaric densities for the model of fullerene obtained from the different versions of GEMC method (*NVT* version, $N = 600$ [10]: x ; *NVT* version, $N = 1500$ [10]: ◇; *NpH* version: o; *μVL* version: Δ). The statistical uncertainties are shown only for the density values (horizontal bars) and only the results of the *NpH* version are joined by the interpolating full lines for clarity purposes.

the vapour phase results were accepted. The calculated temperatures agreed within 1 K in the coexisting phases.

The simulations were checked by the calculated density histograms. The accepted simulations produced histograms with two well separated distribution peaks: no overlaps were found in the density distributions of the coexisting phases.

Three aspects of the methodology became evident during the simulations. First, more than 15 000 cycles were necessary in order to equilibrate the two boxes. This is in contrast with our previous experience for other systems including Lennard-Jones potential [3 – 6], where fewer cycles were necessary, but agrees with our newer observation for square-well fluids. The slow convergence observed also by Caccamo *et al.* [10] can be attributed to the almost hard sphere behaviour followed by a strong attraction of fullerene near contact, which is properly reflected by the present potential model. Second, special care was needed in the *μVL* version to achieve that each subsystem contains reasonable number of particles, since the chemical potential values are very close to each other in the temperature range of interest. Third, using the *NVT* version (with long range corrections) at $T > 1900\,\mathrm{K}$, several identity switches always occured between the two boxes in the course of the simulations. We could get closer to the critical point only by using the *NpH* version; the reason for this is still open to discussion.

We found that the statistical uncertainties obtained by the different versions are nearly equivalent. Although the relative errors of the temperatures of the *NpH* version are smaller than the relative errors of the vapour pressures of the *NVT* version, for this potential model, the possible maximum deviations from the average temperatures in the case of the *NpH* version give rise to similar pressure deviations as observed in the case of the *NVT* version. As far as the μVL version is concerned, besides the vapour pressures also the equilibrium temperatures bear certain errors, but this drawback is partly compensated by the relatively small errors obtained for the temperatures.

In order to estimate the critical temperature (T^c) and the critical density (ρ^c) of the model, the calculated equilibrium liquid (ρ^L) and vapour densities (ρ^V) were fitted to the equations

$$\rho^L = \rho^c + C_2(1 - T/T^c) + B_0(1 - T/T^c)^\beta \tag{6}$$

and

$$\rho^V = \rho^c + C_2(1 - T/T^c) - B_0(1 - T/T^c)^\beta, \tag{7}$$

where C_2 and B_0 are parameters and β is the effective critical exponent. These equations are combinations of the scaling law and the law of rectilinear diameters, where ρ^c and T^c are also regression parameters, and β was taken to be equal to the exact nonclassical value, 0.325. The critical pressure (p^c) was obtained by fitting the vapour pressure data to an equation of the Clausius–Clapeyron form

$$\ln p = A + B/T, \tag{8}$$

where A and B are parameters (see Tab. II). Due to the slightly different estimation method, our prediction for the critical temperature using the results reported by Caccamo *et al.* [10] at $N_{\text{total}} = 600$ is 7 K higher than their's, and this causes limited upward shift of the estimated critical pressure. Although the number of their simulation points at $N_{\text{total}} = 1500$ is insufficient for a correct estimation, it can be seen that the values of

TABLE II Critical properties for the model of fullerene obtained from the different versions of GEMC method

Version	T^c/K	ρ^c/nm^{-3}	p^c/bar
NVT[10]	1934	0.40	30.1
NpH	1952	0.43	32.6
μVL	1947	0.43	32.1

the critical properties would even be higher in that case. The critical temperatures obtained from our simulation results are also higher. It is remarkable that our simulations using the three different GEMC versions yield essentially equivalent vapour–liquid coexistence data and, at higher temperatures, these are in much better agreement with the results for the $N_{\text{total}} = 1500$ case than those for the $N_{\text{total}} = 600$ case. (The literature results for the $N_{\text{total}} = 300$ case, which are not illustrated here, yield still greater deviations). As far as the establishment regarding the existence of a liquid phase of the model is concerned, nevertheless, the discrepancies between the estimated critical properties are small. In all cases, a definite range of temperature can be found where a liquid phase should exist, if we accept the predicted triple point temperature, $T = 1700$ K ± 100 [9, 10].

We suppose that the marked particle number dependence of the results reported by Caccamo *et al.* [10] arise from a conjunction of two sources. The first source is, obviously, the exclusion of the long range corrections from the simulations. The other possible source is the extremely asymmetric particle number distribution employed between the coexisting phases. In order to enhance the convergence of the conventional GEMC runs (*NVT* version), there is an advantage in minimizing the difference between the volumes of the subsystems by using many fewer particles in the dilute phase. It can be avoided by this means that the maximum allowed volume change (in the volume transfer step) would be almost negligible with respect to the volume of the dilute phase. Recently, Valleau [16] showed that if $\langle N^L \rangle > \langle N^V \rangle$, the calculated coexistence densities will be shifted to lower values and this shift will be larger at higher temperatures. Although the magnitude of the effect is unsettled, downward shifts of the predicted critical properties could be expected, as envisaged by Valleau. At $T = 1850$ K, 1880 K and 1890 K, we examined the particle number dependence and particle number distribution dependence by conventional GEMC (*NVT* version) employing exact long range corrections in the simulations. As can be seen in Table I, all the vapour–liquid equilibrium data calculated with different number of particles in the two phases agree far within the statistical uncertainties.

The negligibility of the particle number dependence of our results is reinforced when also the data obtained by the *NpH* and μVL versions ($N_{\mathrm{total}} \approx 500$) are compared with Caccamo's more reliable results at $N_{\mathrm{total}} = 1500$. As far as the asymmetric particle number distribution is concerned, also negligible dependence is shown with the inclusion of the long range corrections.

In our opinion, the use of approximately 100 particles or less, even though in a dilute phase, is generally insufficient for good statistics in molecular simulations. Therefore, at $N_{\mathrm{total}} \approx 500$ we prefer to perform GEMC simulations with nearly equal number of particles in the coexisting phases. The application of the *NpH* version is advantageous in this respect, since an independent choice of the maximum allowed volume changes of the two subsystems is permitted in the uncoupled volume change steps. In this version, the counterpart of the volume transfer step of the *NVT* version is the enthalpy exchange step, but the ratio of the subsystem's enthalpies mostly does not exceed the ratio 2:1 or 3:1 (the ratio of volumes can be even 1:10 or 1:50). Nevertheless, the main advantage of the *NpH* version is the possibility offered to omit the calculation of the virial during the simulation (while the temperature is directly obtained from the value of the potential energy). In the case of the *NVT* version, Harismiadis *et al.* [17] proposed a method for the pressure calculation without evaluating the virial. This would be particularly favourable for complex intermolecular potential functions where the calculation of the virial is computationally expensive, but this also has the drawback associated with the small allowed change of volume during the simulation.

5. CONCLUSION

In this study we focused on the simulation methodology regarding a direct determination of the vapour–liquid coexistence of a fluid with deeply attractive short-ranged potential. In order to make comparisons, we applied all the GEMC versions existing for one-component systems in the literature. Employing exact long range corrections for the potential model of C_{60}, no significant particle number and particle number distribution dependences of the calculated coexistence data were found. According to our experiences for the present model, the GEMC runs lead to satisfactory results with $N_{\mathrm{total}} \approx 500$ particles. As expected, our simulation results confirm that a liquid phase may exist for this model.

References

[1] Panagiotopoulos, A. Z. (1987). "Direct determination of phase coexistence properties of fluids by Monte Carlo simulation in a new ensemble", *Molec. Phys.*, **61**, 813.

[2] Panagiotopoulos, A. Z., Quirke, N., Stapleton, M. and Tildesley, D. J. (1988). "Phase equilibria by simulation in the Gibbs ensemble. Alternative derivation, generalization and application to mixture and membrane equilibria", *Molec. Phys.*, **63**, 527.

[3] Kristóf, T. and Liszi, J. (1996). "Alternative implementations of the Gibbs ensemble Monte Carlo calculation", *Chem. Phys. Lett.*, **261**, 620.

[4] Kristóf, T. and Liszi, J. (1998). "Alternative Gibbs ensemble Monte Carlo implementations: application in mixtures", *Molec. Phys.*, **94**, 519.

[5] Kristóf, T. and Liszi, J. (1997). "Application of a new Gibbs ensemble Monte Carlo method to site-site interaction model fluids", *Molec. Phys.*, **90**, 1031.

[6] Kristóf, T. and Liszi, J. (1997). "Effective Intermolecular Potential for Fluid Hydrogen Sulfide", *J. Phys. Chem.*, **B101**, 5480.

[7] Ashcroft, N. W. (1993). "Elusive diffusive liquids", *Nature*, **365**, 387.

[8] Hagen, M. H. J., Meijer, E. J., Mooij, G. C. A. M., Frenkel, D. and Lekkerkerker, H. N. W. (1993). "Does C_{60} have a liquid phase?", *Nature*, **365**, 425.

[9] Cheng, A., Klein, M. L. and Caccamo, C. (1993). "Prediction of the Phase Diagram of Rigid C_{60} Molecules", *Phys. Rev. Lett.*, **71**, 1200.

[10] Caccamo, C., Costa, D. and Fucile, A. (1997). "A Gibbs ensemble Monte Carlo study of phase coexistence in model C_{60}", *J. Chem. Phys.*, **106**, 255.

[11] Girifalco, L. A. (1992). "Molecular Properties of C_{60} in the Gas and Solid Phases", *J. Phys. Chem.*, **96**, 858.

[12] Panagiotopoulos, A. Z. (1992). "Direct determination of fluid phase equilibria by simulation in the Gibbs ensemble: A review", *Molec. Sim.*, **9**, 1.

[13] Ray, J. R. and Wolf, R. J. (1993). "Monte Carlo simulations at constant chemical potential and pressure", *J. Chem. Phys.*, **98**, 2263.

[14] Guo, M., Peng, D.-Y. and Lu, B. C.-Y. (1997). "On the long-range corrections to computer simulation results for the Lennard-Jones vapour-liquid interface", *Fluid Phase Equilibria*, **130**, 19.

[15] Allen, M. P. and Tildesley, D. J. (1987). *Computer Simulation of Liquids*, Clarendon, Oxford.

[16] Valleau, J. P. (1998). "Number-dependence concerns in Gibbs-ensemble Monte Carlo", *J. Chem. Phys.*, **108**, 2962.

[17] Harismiadis, V. I., Vorholz, J. and Panagiotopoulos, A. Z. (1996). "Efficient pressure estimation in molecular simulations without evaluating the virial", *J. Chem. Phys.*, **105**, 8469.